Comparative Study on Synergistic Effect of LDH and Zirconium Phosphate with Aluminum Trihydroxide on Flame Retardancy of EVA Composites

Ehsan Naderi Kalali [a], Sergio De Juan [a], Xin Wang [a], Shibin Nie [b], Rui Wang [c], De-Yi Wang [a*]

[a] Madrid Institute for Advanced Studies of Materials (IMDEA Materials), C/Eric Kandel, 2, 28906 Getafe, Madrid, Spain
[b] School of Energy Resources and Safety, Anhui University of Science and Technology, 232001 Huainan, Anhui, China
[c] School of Materials Science and Engineering, Beijing Institute of Fashion Technology, 100029, Beijing, China

[*]**Corresponding author:** De-Yi Wang; E-mail: deyi.wang@imdea.org

Abstract

Flame-retardant ethylene vinyl acetate (EVA) composite based on aluminum trihydroxide (ATH), layered double hydroxide (LDH) and organo-modified zirconium phosphate (mZrP) were prepared by melt-compounding method. The synergistic effect of LDH and mZrP with ATH on the fire behavior and thermal stability of EVA composites was studied by limiting oxygen index, UL-94 test, cone calorimeter and thermogravimetric analysis. EVA composite with ATH and LDH passed the V-0 rating while EVA composite with ATH and mZrP exhibited relatively low peak heat release rate. EVA/ATH composite with 10 wt% LDH exhibited a char yield of 34% at 700ºC, while its counterpart with 10 wt% mZrP showed 29%, indicating LDH possessed superior flame retardant synergistic efficiency with ATH over mZrP in terms of promoting char formation. Regarding the heat release rate (HRR), EVA/ATH composite with 10 wt% mZrP displayed a 73% reduction in PHRR, whereas its counterpart with the equivalent loading of LDH showed a lower flame retardant synergistic efficiency (a 58% reduction in peak HRR). The results above demonstrated that LDH mainly functioned as catalyst in char formation, while mZrP was beneficial to restraining heat release.

Keywords

Introduction

Ethylene vinyl acetate (EVA) has been extensively used in wire and cable industry due to its flexibility, toughness and the ability to accept high filler level. These EVA copolymer resins can also meet the needs of electrical applications that require good processing ability, good resistance to environmental stress cracking and excellent heat resistance [1-3]. However, EVA is highly combustible and emits large amount of smoke during combustion. Consequently, EVA needs to be formulated to provide a fire retardant behavior in order to meet the requirements for the wire and cable materials. Traditionally, adding halogenated compounds in combination with antimony trioxide is one of the most efficient and traditional techniques for improving the flame retardancy of polyolefins [4]. Environmental concerns for negative side effects of halogen based fire retardants such as release of optically dense, highly toxic and corrosive smoke [5] demand for the use of halogen-free fire retardants.

In the past few decades, many researchers are focused on exploiting environmental-friendly halogen-free fire retardants for EVA materials. Inorganic fillers, such as magnesium hydroxide (MTH) and aluminum hydroxide (ATH) have been widely applied in flame retardant polymeric materials [6-8]. These fillers could decrease the temperature of the burning materials by endothermic dehydration reaction and release of water vapor into the gas phase to dilute the flame [9]. However, the high loading of inorganic fillers (≈ 60 wt%) is usually required to obtain an satisfactory flame retardancy of EVA composites, which leads to the reduction of

the processing characteristics and deteriorated mechanical properties of the materials [10,11].

New approach has emerged in terms of the combination of classical flame retardants and nanoparticles. In this strategy, classical flame retardant may be ATH or MTH, while nanoparticles include montmorillonite (MMT), layered silicate, and carbon nanotubes (CNTs). The synergistic effect of nanoclay with various flame retardants in EVA has been already investigated. For example, Hull *et al.* [12] described a reinforcement effect of EVA/ATH (40/60 by mass) blends with 5 wt% nanoclays. Peeterbroeck *et al.* [13] and Gao *et al.* [14] studied the synergism between nanoclays and carbon nanotubes in flame retardant EVA composites. A 50% reduction in the PHRR was obtained when 10 wt% of nanoclay was added to EVA [13]. The addition of 2.5 wt% carbon nanotubes associated with 2.5 wt% of nanoclay enhanced the resistance to oxidation of char and decreased the PHRR by 30% compared to pure EVA [14]. These nanocomposites show an enhanced thermal stability and decreased peak heat release rate (PHRR) but, in a number of cases, their mechanical properties have not been mentioned.

In the present work, flame retardant EVA composites were prepared by melt blending, with ATH as flame retardant and layered double hydroxide (LDH) and/or organo-modified zirconium phosphate (mZrP) as synergists. The thermal degradation behaviors of EVA and its composites were studied by thermogravimetric analysis (TG) technique and the flame retardancy of EVA composites were evaluated using cone calorimeter tests (CCTs), UL-94 tests and limiting oxygen index (LOI). Also, the

mechanical properties of EVA and its composites were investigated by tensile tests.

Experimental section

Materials

The EVA copolymer used was a commercial grade Repsol PA-439, with vinyl acetate content of 27% mass fraction and melt flow index of 3.5 g·10 min^{-1}. ATH was obtained from Martinswerk GmbH (Germany). Octacedylamine modified α-zirconium phosphate (mZrP, 57 wt% organic) and Mg-Al LDH were supplied by Prolabin & Tefarm (Italy).

Sample Preparation

The samples were melt-blended via a twin-screw extruder (DSE 20/40 D, Brabender, Germany). The temperature range of the twin-screw extruder was set at 150-175 °C. The formulations are listed in Table 1. The resulting compounds were subsequently dried in an oven at 80°C for 12 h for further injection. The specimens for cone calorimeter (CCT), vertical burning test (UL-94) and mechanical test were prepared by injection molding (Arburg, model: 320 C, Germany, d = 30 mm) under 1500 bar and the temperature profile of 155, 160, 165, 175 and 180 °C.

Table 1. Formulations of EVA-based samples

Characterization

The LOI measurements were carried out using an Oxygen Index model instrument

(Fire Testing Technology, UK) according to ASTM D 2863-97. The sample dimensions were $130 \times 6.5 \times 3.2$ mm^3.

Vertical burning test was conducted on a burning chamber (UL-94, Fire Testing Technology, UK) with the sample dimension of $127 \times 12.7 \times 3.2$ mm^3 according to ASTM D 3801 standard.

Thermogravimeteric analysis (TG) was carried out on a TA-Q50 (TA instrument, USA). Samples mass were approximately 10-20 mg and the runs were carried out in N$_2$, flowing at 90 ml min^{-1}. The heating rate was 10°C min^{-1} over the range of 25-750°C.

The CCTs were performed in a cone calorimeter (Fire Testing Technology, UK) at a heat flux of 50 kW m^{-2} according to ISO 5660 standard. The bottom and edge of each specimen with the dimension of $100 \times 100 \times 4$ mm^3 were wrapped with aluminum foil. All samples were run in duplicate.

The tensile strength and elongation at break were measured on an Instron Universal Tester machine (model 3384) at 25 ± 2°C with a crosshead speed of 6 mm min^{-1}, according to ASTM D 638 standard. Five specimens for each sample were usually analyzed in order to obtain reproducible results and the average value was reported.

Scanning electronic microscopy (SEM) was observed on EVO-MA15 (Zeiss, Germany) to investigating the surface and the cross section of char residues of flame-retardant EVA after CCT test. The surface of the samples was treated by coating a gold layer prior to observation.

Results and Discussion

Tensile Properties

The tensile properties of pure EVA (EVA0) and its composites are given in Table 2. The incorporation of ATH solely has little effect on the tensile strength and the elongation at break of the EVA composite, but improves the Young's modulus due to the rigid nature of ATH filler. In the case of EVA2 and EVA3, adding either mZrP or LDH leads to a remarkable enhancement in Young's modulus (about 81%) and tensile strength (about 65%). The remarkable enhancement is believed to be ascribed to the high aspect-ratio of the nano-fillers. In addition, the incorporation of LDH and/or mZrP decreases the elongation at break of the EVA composites, owing to the intrinsic brittle property of fillers.

Table 2. Tensile test results of the samples

Thermal Analysis

TG curves of pure EVA and its composites are shown in Fig. 1 and the related data is listed in Table 3. The thermal stability was quantified by the initial decomposition temperature that is defined as the temperature where 5% mass is lost ($T_{5\%}$). As it has been demonstrated, EVA0 undergoes two main degradation steps [15]. The first degradation step corresponds to the deacylation reaction associating with the degradation of the acetoxy groups. It occurs in the temperature range from 200 to 350 °C. Previous studies [16] have reported the release of CO, CO_2, H_2O and CH_4 during the first degradation step. The second degradation step is in the temperature

range of 350-500°C, which leads to the formation of polyenes. The dehydrogenated structures produced aromatic volatiles are the origin of char formation. Similarly, all of the EVA composites display a two-step degradation process as pure EVA. As shown in Table 3, the $T_{5\%}$ of the flame retardant EVA composites is decreased compared to pure EVA (EVA0). The reason is probably attributed to the lower decomposition temperature of ATH, mZrP and LDH comparing to EVA, which may accelerate the degradation process. However, the incorporation of fillers improves the residual yield significantly. At 700°C, the amount of the char residues of EVA1, EVA2, EVA3 and EVA4 is 23, 29, 34 and 33%, respectively, which is dramatically higher than EVA0 (0.3%). To confirm the existence of the synergism between different fillers, we assume that there is no interaction between ATH, mZrP and LDH. The char residues of EVA composites at 700°C can be calculated on the basis of the char residue of each component (as listed in Table 3). Based on the results, it can be concluded that EVA3 has relatively higher synergistic efficiency, indicating the existence of good synergism between ATH and LDH.

Table 3. TG data of ATH, mZrP, LDH, EVA and their composites under N_2 atmosphere

Fig. 1 TG curves of EVA and EVA composites under N_2 atmosphere

Flame Retardant Properties of EVA Composites

Table 4 presents the LOI values and UL-94 testing results of the flame retarded EVA composites. It can be observed that the LOI value of sample EVA1 increases to 25.5% from 21.3% for pure EVA. Furthermore, adding mZrP, LDH and mZrP/LDH shows no significant change in LOI value. However, from UL-94 vertical testing test, only EVA3 could pass the V-0 rating. As shown in Fig. 2, in the case of EVA0, fire propagates quickly from igniting with a little char left; for EVA3 sample, no dripping and quick self-extinguishing are observed. The excellent fire resistance of EVA3 could be attributed to the highest char yield as evidenced by TGA that significantly reduces heat transfer and air incursion which enhances the flame-retardant performance of EVA composite.

Table 4. LOI and UL-94 test results of EVA and its composites

Fig. 2 Photos of sample bars after UL-94 test

Cone calorimeter is the most effective method for laboratory evaluation of the fire properties of polymers. The available parameters of the cone calorimeter include: time to ignition (TTI), peak heat release rate (PHRR) and total smoke production (TSP). The heat release rate (HRR) curves measured by cone calorimeter for EVA and its composites are shown in Fig. 3 and the corresponding data are listed in Table 5.

Table 5. Combustion parameters obtained from cone calorimeter

Fig. 3 Heat release rate curves as a function of time of pure EVA and EVA composites

As it is shown in Fig. 3, EVA burns quickly after ignition. A sharp HRR curve appears at the range of 70–230 s with a PHRR value of 1016 kW m^{-2}. The addition of 50 wt% ATH into EVA induces a great reduction in PHRR (57%). Addition of LDH and/or mZrP into the composites leads to a further decrease in the PHRR. Compared to pure EVA, EVA3 shows a PHRR value of 426 kW m^{-2}, whereas EVA2 and EVA4 show more significant reduction in the PHRR value which is 276 and 271 kW m^{-2}, respectively. Usually, the introduction of nano-fillers into the fire retardant polymer systems can improve the char layer's yield [17-20], as shown in Fig. 4, which is responsible for the significant reduction in PHRR.

Fig. 4 Residual mass loss curves of pure EVA and EVA composites

The similar trend can be found in the THR results, as shown in the Fig. 5. At the end of burning, EVA0 shows a total heat of 132.1 MJ m^{-2}, while the THR values of EVA1, EVA2, EVA3 and EVA4 are 126.1, 64.9, 98.2 and 64.8 MJ m^{-2}, respectively.

Fig. 5 Total heat release curves of pure EVA and EVA composites

As shown in Table 5, EVA1 shows little change in TTI compared to the virgin EVA. However, after introducing LDH and mZrP, the TTI value of EVA2, EVA3 and

EVA4 increases to 36, 42 and 46 s respectively, referring to the improvement of the difficult-to-ignite ability of the composites. Moreover, the combustion time of EVA2 and EVA4 is extended to 955 and 1000 s, respectively, from the 465 s of EVA0.

The emission of smoke is regarded as another important parameter in the halogen-free flame retardant materials. The TSR curve is depicted in Fig. 6, and the peak carbon monoxide yield and the peak carbon dioxide yield are summarized in Table 5. It can be observed that both the smoke emission and the carbon oxides yield of EVA composites during combustion process show significant decrease compared to pure EVA, which is attributed to the smoke suppression effect of the nano-fillers.

Fig. 6 Total smoke production curves of pure EVA and EVA composites

Moreover the smoke temperature *versus* time curves of EVA and its composites during the combustion are illustrated in Fig. 7. It is interesting to observe that the smoke temperature of all the EVA composites are lowered comparing to that of pure EVA and introduction of nano-fillers resultes in further reduction of the smoke temperature. Furthermore, mZrP is more effective than LDH as far as the smoke temperature is concerned, which is ascribed to the fact that the increased amount of inflammable gases (*e.g.* CO_2) dilutes the combustion heat feedback to smoke. Fire fatalities by the hot smoke are usually reported as one of the main concerning factors during fire accidents. Therefore, the reduction of the smoke temperature during combustion will be beneficial for fire rescue when an accident happens.

Fig. 7 Smoke temperature vs time curves of pure EVA and EVA composites

Generally, the residual chars formed during combustion can give some important information regarding flame retardant mechanisms to some extent. Therefore, to better understand the char formation of EVA composites and the flame retardant mechanism, the morphology and the structure of the residual chars collected from the cone calorimeter tests were further investigated. The digital photographs of residual chars after cone calorimeter test are displayed in Fig. 8. As can be observed, char residue from EVA1 is bitty and cannot form an effective char layer. In the case of char residue of EVA2, a thermally thick charring residue with lots of cracks and some opening holes is formed. The quality of char layer of EVA3 is slightly improved compared to that of EVA2, still with some opening holes on the surface. In the case of EVA4, after introducing LDH/mZrP mixture in the composite, the quality of char layer is obviously improved with a compact and continuous surface.

Fig. 8 Digital photographs of the residue char after cone calorimeter test: (a) EVA1, (b) EVA2, (c) EVA3 and (d) EVA4.

To further confirm the morphology of the residual chars, SEM was employed to study the exterior and interior chars of the EVA composites, as shown in Fig. 9. For EVA1, the char is bitty and weak with many holes and channels inside. A char with these attributions cannot be a proper thermally insulator. For EVA2, its interior char

seems like a compact cake on the surface whit lots of open holes. EVA2 has a very large char layer and can perform slightly better barrier effect as compared to EVA1. The char of EVA3, similar to the EVA1 is non-continual with lots of open holes on the surface, which cannot inhibit the mass and heat transfer effectively during combustion. The char of EVA4 has a continual and crinkly structure which is similar to the structure of honeycomb. Formation of such a char structure could be attributed to the melt viscosity of the condensed phase which might match the swelling process induced by gas release during combustion. Due to the presence of such intumescing and honeycomb-like char residue, the combustible gases released and heat feedback to the flame are suppressed, and thus great reduction in PHRR, THR and TSP are observed in cone calorimeter tests.

Fig. 9 SEM images of the charred residue after cone calorimeter test: (a) EVA1, (b) EVA2, (c) EVA3 and (d) EVA4

Flame Retardant Mechanism

Based on these results, it is worthy to note that only EVA3 passes UL-94 V-0 testing, but its PHRR is higher compared to EVA2 and EVA4. The possible flame retardant mechanism for different fire retardant EVA composites is proposed, as illustrated in Fig. 10. In the UL-94 tests, the flame is not stable after ignition so that some inflammable pyrolysis gases (*e.g.* water vapor) could easily extinguish the fire. As evidenced by TG, LDH degrades from about 100°C, which is much earlier than mZrP. Therefore, EVA3 shows V-0 rating since the inflammable gases jetting from the early degradation stage of LDH extinguish the fire [21]. For CCTs, the heat flux is much

stronger than UL-94 test, and thus the inflammable gases jetting from the early degradation stage of LDH are not enough to extinguish the fire. From the mass loss curve (Fig. 4), mZrP is more effective to suppress the mass loss rate during combustion than LDH. The reduced mass loss rate is ascribed to the barrier effect of the char layers. After dissecting, a large cavity in char was observed. In fact, the cavity under the char layer can function as gasbag to retard the heat and mass transfer, which is much more effective than the solid char layer. Additionally, EVA2 and EVA4 release much more inflammable gases (*e.g.* CO_2) than EVA3, which dilute the flammable gases during combustion. Therefore, EVA2 and EVA4 show reduced PHRR and THR values compared to EVA3.

Fig. 10 Proposed flame retardant mechanism for fire retardant EVA composites

Conclusions

In this work, the flame retardant EVA and its composites were prepared by the melt blending method, and their morphology, fire behavior, flame retardant mechanism as well as mechanical properties were studied. The results showed that incorporation of mZrP/LDH mixture into EVA/ATH composite resulted in a reduction in thermal stability ($T_{5\%}$), but improved the char yield at 750°C. With 10 wt% of mZrP and/or LDH with 40% ATH, EVA composites exhibited improvement in fire retardancy including the greatly decreased the PHRR, THR, TSP and the enhanced char yield. Addition of mZrP/LDH/ATH significantly increased the tensile strength and the

Young's modulus, but decreased the elongation at break due to the rigid nature of used inorganic fillers. For EVA composites, the flame retardant synergistic efficiency of LDH with ATH was quite different from that of mZrP: LDH was more effective than mZrP in char formation; on the other hand, mZrP showed a 73% reduction in PHRR, which was more efficient than LDH (58% reduction in PHRR). These phenomena could be explained by different roles of LDH and mZrP on the flame retardancy of EVA composites: LDH mainly functioned as catalyst in char formation, while mZrP probably promoted the release of inflammable gases (*e.g.* CO_2) during combustion. The formulations presented herein of the flame retardant EVA composites based on mZrP/LDH/ATH have promising potential application in wire and cable industry.

Acknowledgement

References

1. Li L, Qian Y, Jiao C. M. Synergistic flame retardant effect of melamine in ethylene–vinyl acetate/layered double hydroxides composites. J. Therm. Anal. Calorim . 2013, 114;45-55.

2. Beyer G. Flame retardant properties of EVA-nanocomposites and improvements by combination of nanofillers with aluminium trihydrate. Fire Mater. 2001, 25, 193-7.

3. Nistor M.T., Vasile C. Influence of the nanoparticle type on the thermal decomposition of the green starch/poly(vinyl alcohol)/montmorillonite nanocomposites. J. Therm. Anal. Calorim. 2013, 111; 1903-1919

4. Yin H.Q, Yuan D.D, Cai X.F. Red phosphorus acts as second acid source to form a novel intumescent-contractive flame-retardant system on ABS. J. Therm. Anal. Calorim. 2013, 111; 499-506.

5. Wang X, Hu Y, Song L, Xing WY, Lu HD, Lv P, Jie GX. Flame retardancy and thermal degradation mechanism of epoxy resin composites based on a DOPO substituted organophosphorus oligomer. Polymer 2010, 51, 2435-45.

6. Sener AA, Demirhan E. The investigation of using magnesium hydroxide as a flame retardant in the cable insulation material by cross-linked polyethylene. Mater. Design 2008, 29, 1376-9.

7. Bahattab MA, Mosnacek J, Basfar AA, Shukri TM. Cross-linked poly (ethylene vinyl acetate)(EVA)/low density polyethylene (LDPE)/metal hydroxides composites for wire and cable applications. Polym. Bull. 2010, 64, 569-80.

8. Rybiński P, Janowska G. Effect of halogenless flame retardants on the thermal properties, flammability, and fire hazard of cross-linked EVM/NBR rubber blends. J. Therm. Anal. Calorim. 2014, 115; 771-782

9. Rychly J, Vesely K, Gal E, Kummer M, Jancar J, Rychla L. Use of thermal methods in the characterization of the high-temperature decomposition and ignition of polyolefins and EVA copolymers filled with $Mg(OH)_2$, $Al(OH)_3$ and $CaCO_3$. Polym. Degrad. Stabil. 1990, 30, 57-72.

10. LeBaron PC, Wang Z, Pinnavaia TJ. Polymer-layered silicate nanocomposites: an overview. Appl. Clay Sci. 1999, 15, 11-29.

11. Porter D, Metcalfe E, Thomas M. Nanocomposite fire retardants—a review. Fire Mater. 2000, 24, 45-52.

12. Hull TR, Price D, Liu Y, Wills CL, Brady J. An investigation into the decomposition and burning behaviour of ethylene-vinyl acetate copolymer nanocomposite materials. Polym. Degrad. Stabil. 2003, 82, 365-71.

13. Peeterbroeck S, Alexandre M, Nagy J, Pirlot C, Fonseca A, Moreau N, Philippin G, Delhalle J, Mekhalif Z, Sporken R. Polymer-layered silicate–carbon nanotube nanocomposites: unique nanofiller synergistic effect. Compos. Sci. Technol. 2004, 64, 2317-23.

14. Gao F, Beyer G, Yuan Q. A mechanistic study of fire retardancy of carbon nanotube/ethylene vinyl acetate copolymers and their clay composites. Polym. Degrad. Stabil. 2005, 89, 559-64.

15. Allen NS, Edge M, Rodriguez M, Liauw CM, Fontan E. Aspects of the thermal oxidation of ethylene vinyl acetate copolymer. Polym. Degrad. Stabil. 2000, 68, 363-71.

16. Marcilla A, Gomez-Siurana A, Menargues S. Oxidative degradation of EVA copolymers in the presence of catalysts. J. Therm. Anal. Calorim. 2007, 87, 519-27.

17. Wang DY, Leuteritz A, Wang YZ, Wagenknecht U, Heinrich G. Preparation and burning behaviors of flame retarding biodegradable poly(lactic acid)

nanocomposite based on zinc aluminum layered double hydroxide. Polym. Degrad. Stabil. 2010, 95, 2474-80.

18. Wang DY, Song YP, Lin L, Wang XL, Wang YZ. A novel phosphorus-containing poly(lactic acid) toward its flame retardation. Polymer 2011, 52, 233-8.

19. Wang X, Hu Y, Song L. Xing WY, Lu HD. Thermal degradation behaviors of epoxy resin/POSS hybrids and phosphorus–silicon synergism of flame retardancy. J. Polym. Sci. Polym. Phys. 2010, 48, 693-705.

20. Wang X, Song L, Yang HY, Xing WY, Kandola B, Hu Y. Simultaneous reduction and surface functionalization of graphene oxide with POSS for reducing fire hazards in epoxy composites. J. Mater. Chem. 2012, 22, 22037-43.

21. Zhang WC, Li XM, Yang RJ. Blowing-out effect and temperature profile in condensed phase in flame retarding epoxy resins by phosphorus-containing oligomeric silsesquioxane. Polym. Advan. Technol. 2013, 24, 951-61.
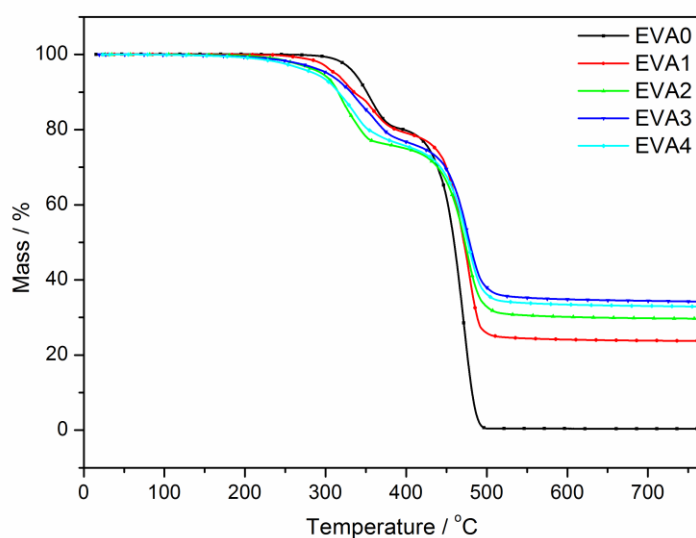
Figure 1 TG curves of EVA and EVA composites under N2 atmosphere
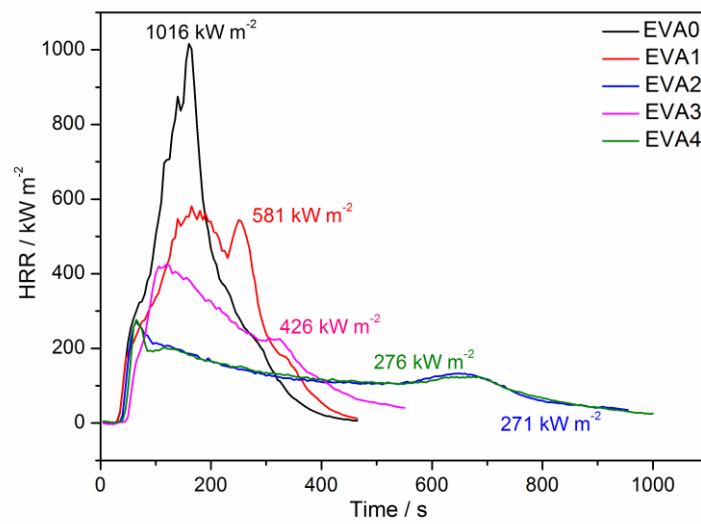
Figure 2 Photos of sample bars after UL-94 test

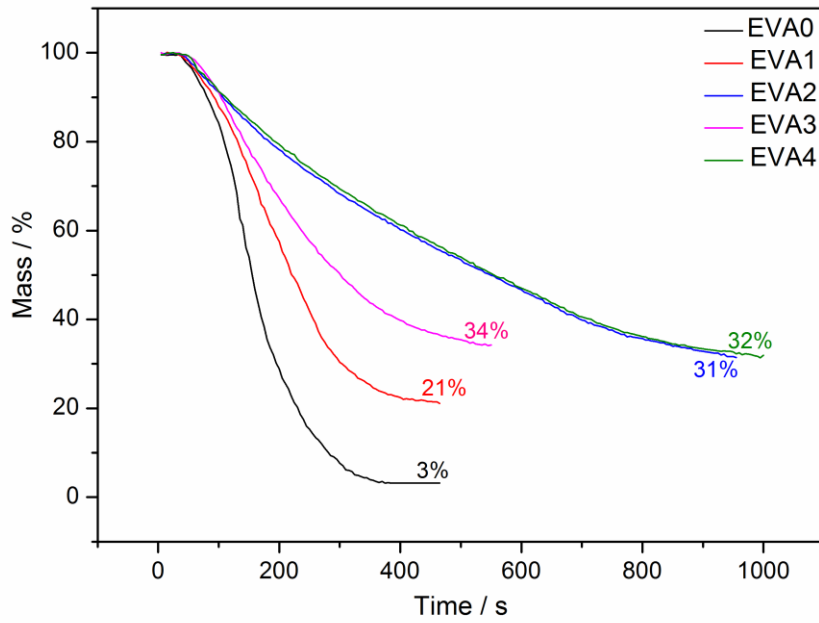**Figure 3 Heat release rate curves as a function of time of pure EVA and EVA composites**

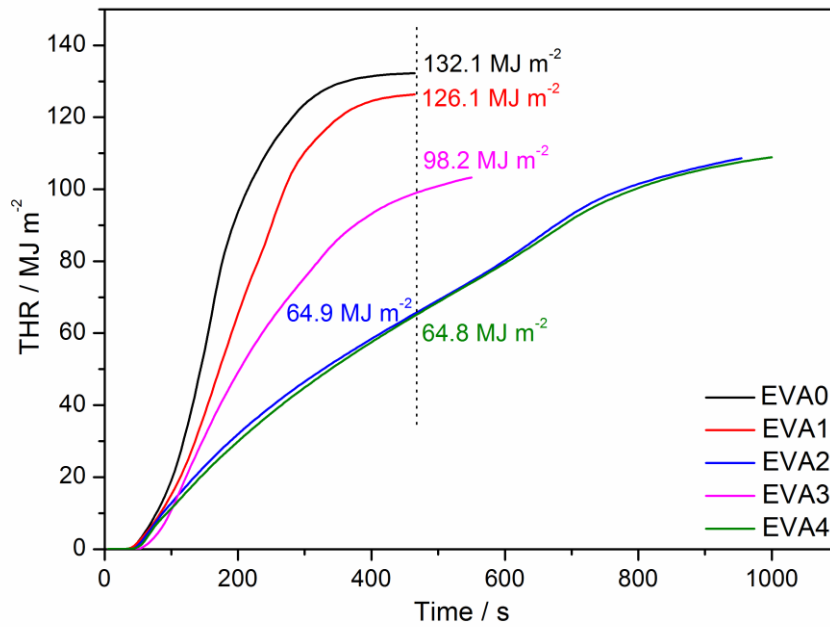**Figure 4 Residual mass loss curves of pure EVA and EVA composites**

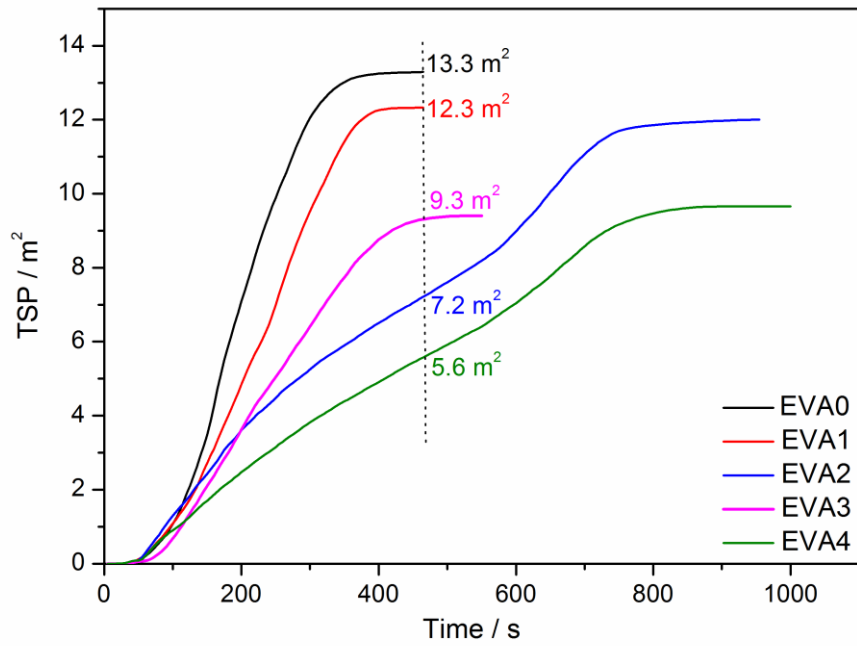**Figure 5 Total heat release curves of pure EVA and EVA composites**

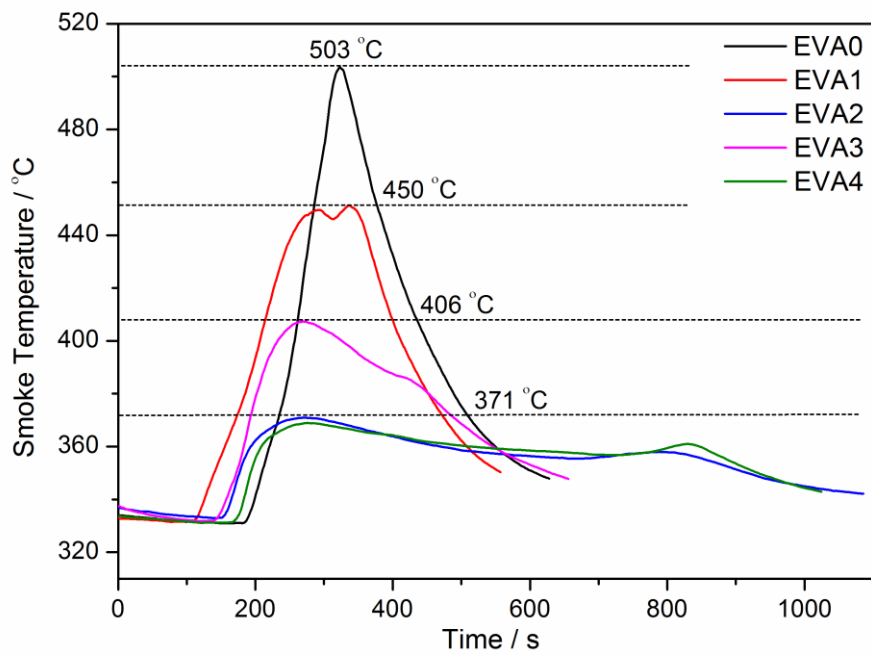**Figure 6 Total smoke production curves of pure EVA and EVA composites**

Figure 7 Smoke temperature vs time curves of pure EVA and EVA composites
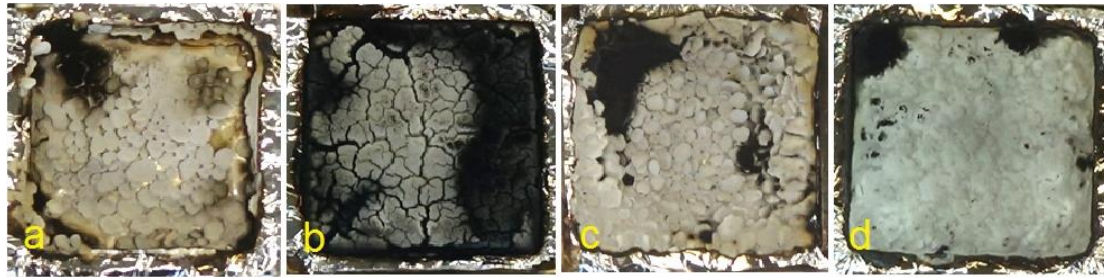
Figure 8 Digital photographs of the residue char after cone calorimeter test, (a) EVA1, (b) EVA2, (c) EVA3 and (d) EVA4
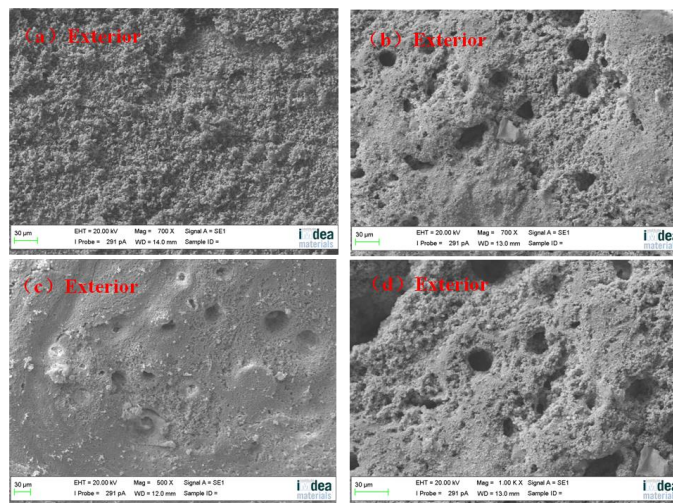

Figure 9 SEM images of the charred residue after cone calorimeter test: (a) EVA1, (b) EVA2, (c) EVA3 and (d) EVA4
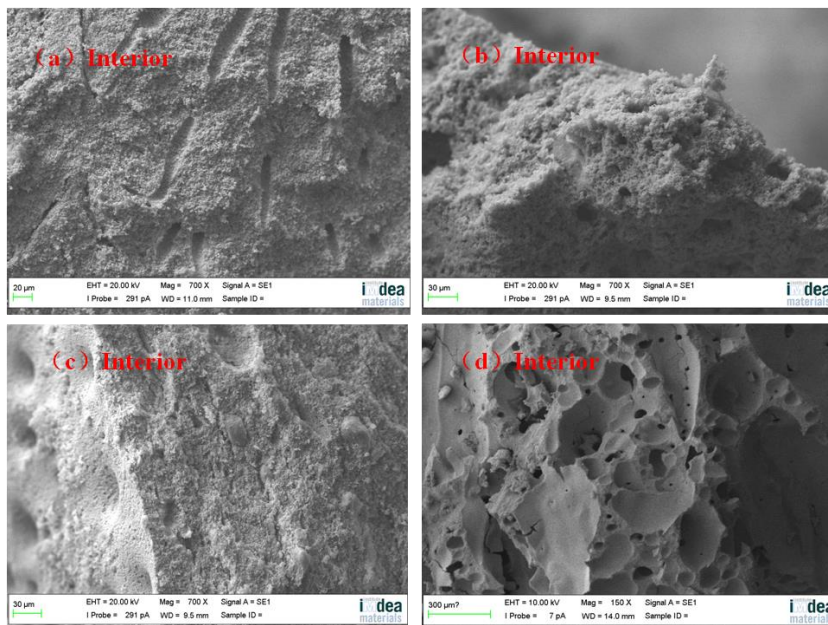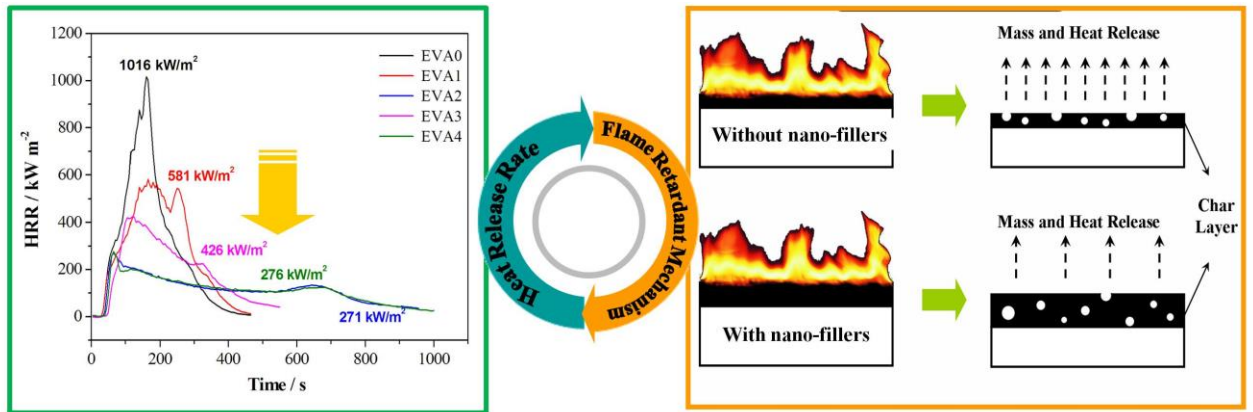

Figure 10 Proposed flame retardant mechanism for fire retardant EVA composites

Sample	EVA / %	ATH / %	mZrP / %	LDH / %
EVA0	100	-	-	-
EVA1	50	50	-	-
EVA2	50	40	10	-
EVA3	50	40	-	10
EVA4	50	40	5	5

Table 1 Formulations of EVA-based samples

Sample	Tensile Strength / MPa	Elongation at break / %	Young's modulus / MPa
EVA0	3.5 ± 0.5	176.6 ± 10.7	10.2 ± 0.5
EVA1	3.9 ± 0.4	178.5 ± 18.4	26.7 ± 2.4
EVA2	10.1 ± 0.4	100.7 ± 4.7	62.1 ± 6.3
EVA3	10.7 ± 0.1	110.0 ± 13.5	69.1 ± 1.6
EVA4	9.6 ± 0.9	101.0 ± 2.7	54.9 ± 9.6

Table 2 Tensile test results of the samples

Sample	$T_{5\%}$ / °C	Residual yield at 700°C / wt%	
		Experimental	Calculated
ATH	245	65	-
mZrP	205	42	-
LDH	97	53	-
mZrP/LDH (1:1)	138	48	-
EVA0	335	0.3	-
EVA1	311	23	32
EVA2	294	29	30
EVA3	301	34	31
EVA4	285	33	31

Table 3 TGA data of ATH, mZrP, LDH, EVA and their composites under N2 atmosphere

Sample	LOI / %	UL-94	Observation
EVA0	21.3	No rating	Fail, flame dripping
EVA1	25.5	V-2	Fail, flame dripping
EVA2	25.0	No rating	Fail, flame dripping
EVA3	25.0	V-0	No fire, No dripping
EVA4	25.0	No rating	Fail, flame dripping

Table 4 LOI and UL-94 test results of EVA and its composites

Sample	TTI / s	PHRR / kW m^{-2}	THR / MJ m^{-2}	Time to flame out / s	Peak of CO / kg kg^{-1}	Peak of CO$_2$ / kg kg^{-1}
EVA0	32	1016	132.1	465	32.9	1253.4
EVA1	33	581	126.1	465	14.0	824.4
EVA2	36	271	64.9	955	0.6	23.8
EVA3	46	426	98.2	550	0.1	5.5
EVA4	42	276	64.8	1000	0.8	15.2

Table 5 Combustion parameters obtained from cone calorimeter.